

Enhancing IMU-Based Online Handwriting Recognition via Contrastive Learning with Zero Inference Overhead

Jindong Li^{1,4[0000-0002-3550-1660]}, Dario Zanca^{1[0000-0001-5886-0597]}, Vincent Christlein^{1[0000-0003-0455-3799]}, Tim Hamann^{2[0000-0003-3562-6882]}, Jens Barth^{2[0000-0003-3967-9578]}, Peter Kämpf², and Björn Eskofier^{1,3,4,5[0000-0002-0417-0336]}

¹ Friedrich-Alexander-Universität Erlangen-Nürnberg, Erlangen, Germany

² STABILO International GmbH, Heroldsberg, Germany

³ Ludwig-Maximilians-Universität München, Munich, Germany

⁴ Munich Center for Machine Learning, Munich, Germany

⁵ Helmholtz Zentrum München - German Research Center for Environmental Health, Neuherberg, Germany

Abstract. Online handwriting recognition using inertial measurement units opens up handwriting on paper as input for digital devices. Doing it on edge hardware improves privacy and lowers latency, but entails memory constraints. To address this, we propose Error-enhanced Contrastive Handwriting Recognition (ECHWR), a training framework designed to improve feature representation and recognition accuracy without increasing inference costs. ECHWR utilizes a temporary auxiliary branch that aligns sensor signals with semantic text embeddings during the training phase. This alignment is maintained through a dual contrastive objective: an in-batch contrastive loss for general modality alignment and a novel error-based contrastive loss that distinguishes between correct signals and synthetic hard negatives. The auxiliary branch is discarded after training, which allows the deployed model to keep its original, efficient architecture. Evaluations on the OnHW-Words500 dataset show that ECHWR significantly outperforms state-of-the-art baselines, reducing character error rates by up to 7.4% on the writer-independent split and 10.4% on the writer-dependent split. Finally, although our ablation studies indicate that solving specific challenges require specific architectural and objective configurations, error-based contrastive loss shows its effectiveness for handling unseen writing styles. Code is available at: <https://anonymous.4open.science/r/ECHWR>.

Keywords: Online Handwriting Recognition · Time-Series Analysis · Contrastive Learning

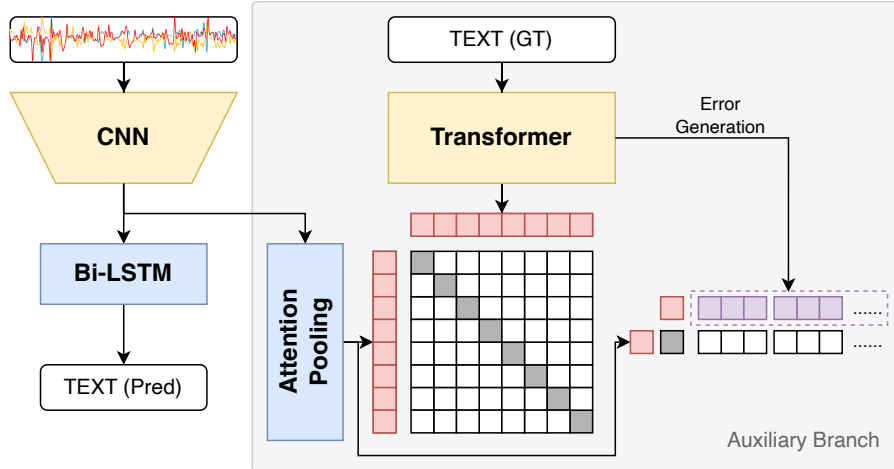


Fig. 1. The ECHWR framework. The model trains a primary sensor branch (left) jointly with an auxiliary text branch to align feature representations. The training objective combines CTC loss with two contrastive components: an in-batch contrastive loss (middle) to align matching sensor-text pairs and a novel error-based contrastive loss (right) to discriminate against synthetic “hard negatives.” The auxiliary branch is removed during inference to maintain zero computational overhead.

1 Introduction

Handwriting remains a highly natural and efficient form of human communication. This makes online handwriting recognition (OnHWR), particularly inertial measurement unit (IMU)-based systems, a critical interface for modern smart devices. Because dynamic handwriting data contains unique biometric traits that can reveal sensitive user information [6,27], users are often hesitant to transmit raw sensor trajectories to cloud servers. However, executing recognition locally imposes strict computational limits. While large-scale models offer high accuracy, they are frequently unsuitable for edge devices due to latency and memory constraints. Consequently, there is a critical need for efficient OnHWR approaches that maintain high performance while staying within the hardware capabilities of portable electronics.

Meeting these privacy, latency, and memory constraints is difficult with existing methods. Although modern encoder-decoder models achieve high performance, they often rely on complex architectures that result in high latency [25,15,16]. In resource-constrained environments, simply increasing model size to improve feature extraction is impractical. Therefore, we require training strategies that extract richer information from sensor data without increasing the computational load during inference.

Contrastive learning has become a standard technique in computer vision [2,21] for learning robust features by aligning similar representations, and this

success has extended to time-series analysis [5]. However, these methods typically use contrastive learning only for pre-training. In sequence recognition tasks, such as speech or IMU-based handwriting recognition, models rarely combine contrastive objectives with the primary supervised loss during end-to-end training. As a result, the potential for contrastive learning to enhance feature quality directly during the main training phase remains largely unexplored.

To bridge this gap, we propose ECHWR, as shown in Fig. 1. This training framework improves IMU-based OnHWR accuracy with zero inference overhead. Unlike standard methods that use only connectionist temporal classification (CTC) loss, we introduce a temporary auxiliary branch that embeds ground-truth text using a Transformer encoder. We then align sensor and text representations through a dual contrastive objective. First, an in-batch contrastive loss aligns matching sensor-text pairs while treating other pairs in the batch as negatives. Second, a novel error-based contrastive loss forces the model to distinguish correct transcripts from “hard negatives,” which are artificially generated texts containing random errors such as deletions, insertions, or substitutions. Crucially, we discard the auxiliary branch after training. This approach allows the primary IMU-based OnHWR model to learn richer features and achieve higher accuracy without increasing computational costs or altering the architecture during deployment.

2 Related Works

2.1 IMU-Based OnHWR

Early IMU-based handwriting recognition relied heavily on manual feature engineering and statistical modeling. Researchers typically employed sensor fusion techniques, such as quaternion-based complementary filters, to reconstruct motion trajectories from raw accelerometer and gyroscope signals [8]. Dynamic time warping served as the standard approach for handling temporal variations in isolated characters [8,9]. For more complex sequences, probabilistic models like hidden Markov models were used for both character classification [3] and continuous text spotting in 3D space [1]. Despite their utility, these methods often struggled with sensor noise, sensor bias and the significant variability found in individual writing styles.

The advent of deep learning shifted the focus toward end-to-end neural networks that extract features directly from raw data. Architectures combining convolutional neural networks (CNNs) and Long Short-Term Memory (LSTM) networks became the standard for capturing spatial and temporal dependencies. By using CTC loss, these models align unsegmented sensor streams to text, which enables robust word and sentence recognition [24,19]. More recently, research has shifted toward efficiency. This includes exploring lightweight architectures and specialized training strategies designed to maintain high performance without the heavy computational costs typically associated with deep models [14].

2.2 Contrastive Learning

Modern representation learning relies heavily on instance discrimination tasks. Methods such as SimCLR [2] and CLIP [21] use the InfoNCE loss to maximize agreement between different versions of the same image while increasing the distance from other samples in the batch. By optimizing this objective, these frameworks encourage the model to learn features that remain consistent across transformations but are still distinct enough to tell different instances apart. These strategies primarily focus on spatial consistency and global alignment to create robust visual models.

In the time-series domain, researchers have adapted these objectives to capture temporal dynamics. For example, TS-TCC [5] and other pre-training frameworks [28,13,12] typically enforce consistency between different augmentations or time-frequency views of a signal. These methods generally treat contrastive learning as a standalone pre-training phase used to initialize encoder weights. In contrast, joint optimization strategies are still rare. While a few studies in spatio-temporal forecasting [17] and human activity recognition [7] have used contrastive loss as an auxiliary regularizer, these works focus on classification rather than sequence-to-sequence recognition tasks.

Regardless of the domain, the effectiveness of contrastive objectives depends heavily on the sampling strategy. Traditional approaches that use random “in-batch” negatives often face the issue of vanishing gradients, as the model can easily distinguish the majority of negative pairs. Research in hard negative mining [10,11,22] shows that prioritizing difficult samples prevents the model from learning simple or trivial solutions. By focusing on samples that are semantically different yet close in the embedding space, these methods force the encoder to learn more detailed and discriminative features.

3 Methods

3.1 Model Architecture

The ECHWR framework is built upon the REWI [14], which is the state-of-the-art model for IMU-based OnHWR. This model follows an encoder-decoder architecture, where the encoder is a CNN and the decoder is a network based on bidirectional LSTM.

To improve the feature representation of the CNN backbone without changing its structure for inference, we add a temporary auxiliary branch. This branch aligns sensor signals with semantic text embeddings and consists of a dedicated text encoder and an attention pooling module to bridge the difference in dimensionality between the time-series sensor features and the text representations. During training, the model is regularized by two auxiliary objectives: an in-batch contrastive loss to align sensor and text representations, and a novel error-based contrastive loss to help the model distinguish against hard artificial negative samples. Importantly, the entire auxiliary branch is discarded after training. This ensures that the deployed model keeps the original REWI architecture and operates with no additional computational costs.

Attention Pooling The attention pooling layer aligns the variable-length sensor sequence with the text embedding. First, the primary CNN encoder produces a temporal sequence of features $X \in \mathbb{R}^{T \times D_{in}}$, where T represents the sequence length. The module then linearly projects these features to a target dimension D_{out} of 512. Standard sinusoidal positional embeddings are added at this stage to preserve the temporal order of the data.

Finally, a Multi-Head Attention mechanism with 8 heads is applied. In this step, the mean of the projected sequence serves as the *query* (Q), while the entire sequence serves as both the *keys* (K) and *values* (V). This process aggregates relevant sensor segments into a single global token, resulting in a fixed-length context vector $c_{sig} \in \mathbb{R}^{D_{out}}$ for contrastive alignment.

Text Encoder The text encoder generates semantic embeddings from both ground-truth and hard negative transcripts. We employ a lightweight Transformer with three encoder layers [23], configured with 8 attention heads, a model and embedding dimension of 512, and an attention dropout rate of 0.1. The encoder operates at the character level, treating each character as an individual token to match the fine-grained nature of handwriting. To capture spatial relationships, learnable position embeddings are added to the token embeddings. We also prepend a learnable [CLS] token to the input sequence to aggregate global context. The final output vector of this token serves as the global text embedding z_{text} . This encoder is trained from scratch in conjunction with the sensor network.

Embedding Improvement Since embedding quality is essential for contrastive learning, we investigate the effect of the gated attention mechanism [20], registers [4], and root mean square (RMS) normalization [26] on feature representation. While the first two methods originate from large language models and computer vision, respectively, they both address the issue of attention artifacts. The gated attention mechanism adds a gating factor to the attention formulation. This allows the model to focus on informative features while suppressing noise. Registers are auxiliary learnable tokens added to the input sequence that act as “sinks” for global information. This prevents the model from repurposing semantic tokens for global reasoning. Additionally, we employ RMS normalization to improve training stability and representation quality. We apply head-wise gated attention to both the attention pooling layer and the text Transformer encoder, whereas RMS normalization and registers are only used within the text Transformer.

3.2 Training Objective

As shown in Eq. 1, we use a composite objective function designed to jointly optimize handwriting recognition accuracy and semantic representation alignment. It integrates a smoothed CTC loss adopted from REWI [14], with two distinct contrastive mechanisms. Specifically, we employ an in-batch contrastive (BC) loss

to align time-series and textual modalities, and an Error-based contrastive (EC) loss to help the model distinguish ground-truth text from hard negative errors.

$$\mathcal{L}_{total} = \mathcal{L}_{CTC} + \mathcal{L}_{BC} + \mathcal{L}_{EC} \quad (1)$$

In-Batch Contrastive Loss The BC loss aligns the latent representations of time-series sensor data with their corresponding textual transcripts. Given a batch of N sensor-text pairs, let $c_{sig}^{(i)}$ and $z_{text}^{(i)}$ represent the normalized sensor and text embeddings for the i -th sample. The similarity between a sensor embedding and a text embedding is computed as $s_{i,j} = \tau \cdot (c_{sig}^{(i)\top} z_{text}^{(j)})$, where τ is a learnable scaling parameter. The loss is then calculated symmetrically as follows:

$$\mathcal{L}_{BC} = -\frac{1}{2N} \sum_{i=1}^N \left(\log \frac{\exp(s_{i,i})}{\sum_{j=1}^N \exp(s_{i,j})} + \log \frac{\exp(s_{i,i})}{\sum_{j=1}^N \exp(s_{j,i})} \right) \quad (2)$$

To avoid false negatives caused by identical transcripts, we filter the batch to ensure that each unique text label appears only once.

Error-Based Contrastive Loss The EC loss forces the model to distinguish ground-truth text from artificial hard negatives. For each sample i , we generate S sets of hard negatives. Each set contains three variants that correspond to single-character deletion, insertion, or substitution errors. This process results in a total of $M = 3S$ negative samples $\{z_{text}^{(i,k)}\}_{k=1}^M$, all of which have a Levenshtein distance of one from the ground truth $z_{text}^{(i,0)}$. The loss is computed as follows:

$$\mathcal{L}_{EC} = -\frac{1}{N} \sum_{i=1}^N \log \frac{\exp(\tau \cdot c_{sig}^{(i)\top} z_{text}^{(i,0)})}{\sum_{k=0}^M \exp(\tau \cdot c_{sig}^{(i)\top} z_{text}^{(i,k)})} \quad (3)$$

This objective compels the model to learn fine-grained features. These features are necessary to accurately discriminate between highly similar transcripts that differ by only a single character.

4 Experiments

4.1 Datasets

We utilize the right-handed subset of the OnHW-Words500 dataset [19], which contains 13-channel handwriting data collected from 53 subjects using a sensor-enhanced pen developed by STABILO International GmbH. This dataset is provided with two distinct evaluation protocols: writer-dependent (WD) and writer-independent (WI), which represent splits by words and by writers, respectively, using 5-fold cross-validation. We employ both splits to evaluate the model against different distribution shifts between the training and test sets, which include character distribution variations, as illustrated in Appx. A, and differences in individual handwriting styles.

4.2 Implementation Details

We adopt the core architecture from REWI [14]. Following a similar setup, we train the model for 300 epochs with a batch size of 64. The training process employs a learning rate schedule consisting of a 30-epoch linear warmup followed by cosine annealing. We use the AdamW optimizer with a weight decay of 10^{-2} . For the primary OnHWR backbone, we set the learning rate to 10^{-3} , whereas we use a lower learning rate of 2.5×10^{-4} for the auxiliary contrastive branch to ensure training stability. The framework is implemented using PyTorch 2.9.1 on an NVIDIA RTX 3090 GPU with 24 GB of VRAM.

Performance is evaluated at two levels of granularity. character error rate (CER) measures errors at the character level, and word error rate (WER) assesses them at the word level. These metrics quantify the total number of substitutions, deletions, and insertions required to align the model’s predictions with the ground truth.

4.3 Objective Analysis

To rigorously assess the effectiveness of the ECHWR framework, we compared it against the REWI baseline across different model sizes and objective configurations, as shown in Table 1.

Table 1. Objective Analysis. The WD split results utilize the *RMSNorm + Gated Attention* architecture, while the WI split utilizes the *LayerNorm + Gated Attention + Registers* architecture.

Objectives			WD		WI	
CTC	BC	EC	CER (%)	WER (%)	CER (%)	WER (%)
<i>ECHWR/S</i>						
✓			15.99	51.17	10.24	24.55
✓	✓		15.59	50.28	10.61	25.47
✓	✓	✓	15.99	50.77	10.59	25.18
<i>ECHWR/B</i>						
✓			14.45	43.96	7.33	15.16
✓	✓		12.95	40.26	7.03	14.31
✓	✓	✓	14.04	41.99	6.79	13.65

On the WD split, where the model encounters unseen words from known writers, the BC objective is the decisive factor. For the base architecture ECHWR/B, adding the BC objective alone reduces the CER and WER to 12.95% and 40.26%, respectively. This represents a relative improvement of 10.4% (1.5 pp) for CER and 8.4% (3.7 pp) for WER over the baseline. Notably, this configuration outperforms the variant that includes the EC objective. This suggests that when writing styles are familiar but the vocabulary is novel, the primary challenge is

aligning sensor signals to character representations rather than identifying complex noise. The BC objective addresses this by enforcing a flexible alignment between sensor and text embeddings. In contrast, the EC objective appears to create a rigidity that hinders the model’s ability to generalize to the novel character sequences in the WD split.

Conversely, the WI split benefits from the stricter decision boundaries enforced by the EC objective. While adding BC provides a strong foundation, improving the baseline CER from 7.33% to 7.03% and WER from 15.16% to 14.31%, the full configuration with EC yields the best performance at 6.79% and 13.65%. This marks 7.4% (0.54 pp) and 10.0% (1.51 pp) relative CER and WER improvement over the baseline. When facing known words written by unknown subjects, the primary source of error is often ambiguity caused by biometric variance. The EC objective forces the model to reject “hard negatives” (e.g., single character substitutions), effectively cutting through the noise of unfamiliar writing styles to maximize precision on known vocabulary.

Overall, the proposed ECHWR framework demonstrates consistent gains over the REWI baseline across different tasks, though these benefits are constrained by model capacity. For the standard Base model (ECHWR/B), our method achieves robust improvements on both generalization fronts. This confirms that enforcing alignment between sensor signals and text embeddings allows the primary backbone to learn more robust features without increasing inference complexity. However, lacking sufficient parameters, the small encoder appears saturated by the dual burden of minimizing the CTC loss while simultaneously optimizing auxiliary contrastive objectives, resulting in negligible gains or slight underfitting compared to its baseline.

4.4 Architectural Analysis

To understand the mechanisms driving the performance gains, we analyze the impact of normalization and representation enhancement strategies. Table 2 details the performance of these variants. Rather than a single universal architecture, the results reveal distinct structural preferences for different generalization tasks.

The comparison between layer normalization and RMS normalization highlights a trade-off between feature stability and robustness. The WD split, which involves known writers but unseen vocabulary, consistently favors variants with RMS normalization. By normalizing only the scale and not the centering, RMS normalization preserves more of the original feature variance. This property is crucial when the model must construct novel words from known character patterns, as it maintains the subtle variance required for fine-grained sequence composition.

In contrast, the WI split, dominated by the noise of unseen handwriting styles, benefits from the stricter standardization of layer normalization. This method forces every sample into a unified distribution, effectively normalizing away global shifts in writer style. This creates a more robust feature space for

Table 2. Architectural Analysis of ECHWR Variants. We investigate the impact of various normalization strategies alongside the inclusion of head-wise gated attention (GA) and register tokens (Reg). This analysis is conducted using the ECHWR/B model under the supervision of different training objectives.

Variants	Objectives				WD		WI		
	GA	Reg	CTC	BC	EC	CER (%)	WER (%)	CER (%)	WER (%)
REWI/B	✓					14.45	43.96	7.33	15.16
<i>LayerNorm Variants</i>									
	✓	✓				13.66	41.51	7.00	13.93
	✓	✓	✓			13.81	41.74	7.10	14.31
✓	✓	✓	✓			14.51	42.52	6.93	13.98
✓	✓	✓	✓	✓		13.94	41.82	6.88	13.74
✓	✓	✓	✓	✓		13.71	41.3	7.03	14.31
✓	✓	✓	✓	✓	✓	14.27	42.18	6.79	13.65
<i>RMSNorm Variants</i>									
	✓	✓				13.69	41.31	6.85	13.88
	✓	✓	✓			13.82	41.58	6.94	14.22
✓	✓	✓	✓			12.95	40.26	6.80	14.15
✓	✓	✓	✓	✓		14.04	41.99	7.00	13.96
✓	✓	✓	✓	✓		13.20	40.57	6.91	14.25
✓	✓	✓	✓	✓	✓	13.71	41.67	6.86	13.93

the contrastive loss, preventing the model from overfitting to writer-specific idiosyncrasies.

The addition of gated attention generally acts as a signal sharpener. Across most RMS configurations, gated attention improves performance by dynamically suppressing background noise in the sensor and text embeddings before alignment. This is particularly effective in the WD split, where the “RMSNorm + Gated Attention” combination yields the most significant gains. It ensures that only high-quality visual features contribute to the alignment loss without forcing a centered representation.

The role of registers is highly context-dependent. They provide no benefit and often degrade performance on the WD split, likely by introducing unnecessary capacity that the model struggles to optimize for known writers. However, for the WI split, the combination of “LayerNorm + Gated Attention + Registers” is essential for achieving the state-of-the-art. This supports the hypothesis that registers serve as “style sinks.” They absorb attention noise from the text representation, which is especially useful when texts are short and the representation might otherwise be dominated by artifacts.

4.5 Error Set Size Analysis

To identify the optimal balance between sample diversity and training stability, we investigate how the proposed framework responds to the number of hard neg-

ative samples. This analysis is conducted across various ECHWR configurations, with the results illustrated in Fig. 2.

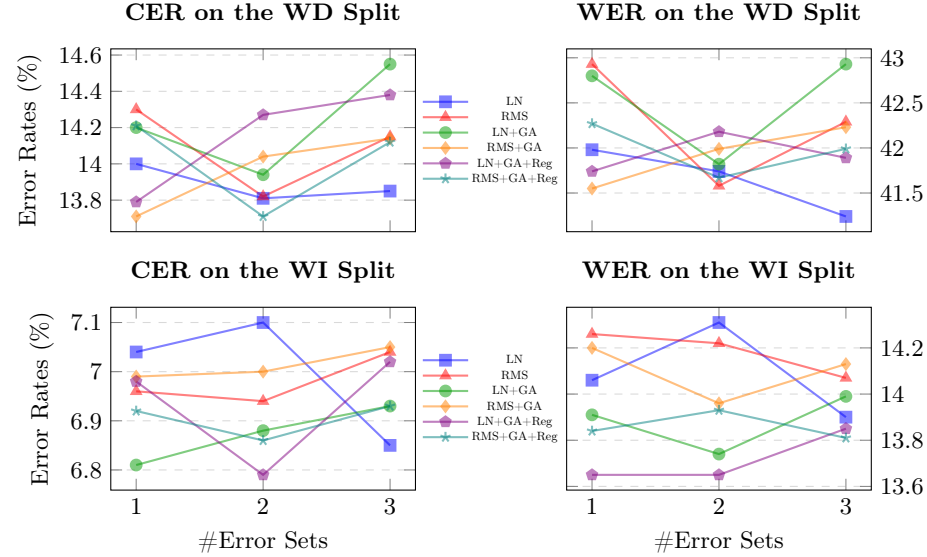


Fig. 2. Sensitivity to Negative Sample Diversity. The plots show performance changes across different error set sizes. The central legend applies to all subplots.

Across most architectural configurations, an error set size of two emerges as the most effective setting. On both the WD and WI splits, we observe a general trend where performance improves significantly when increasing the number of error sets from one to two. However, accuracy often plateaus or declines when increasing the count to three.

The results reveal an interesting relationship between architectural complexity and the need for negative samples. Simpler models often show continued improvement or stability with three error sets. Because they lack sophisticated attention filtering, these models seem to benefit from the stronger data augmentation provided by a larger quantity of hard negatives. In contrast, models equipped with gated attention or registers tend to peak at two error sets. Since these mechanisms are already efficient at suppressing noise and focusing on informative features, adding more negative samples yields diminishing returns. Therefore, we use an error set size of two as the standard configuration for ECHWR.

4.6 Qualitative Analysis

To empirically validate the impact of the contrastive objectives, we visualize the learned embedding space using UMAP [18]. We extract embeddings from the

validation sets of the first fold using the optimal configurations: *RMSNorm + Gated Attention* for the WD split and *LayerNorm + Gated Attention + Registers* for the WI split. Figure 3 presents the projections of sensor sequences, ground-truth text anchors, and generated hard negative errors for three sample words.

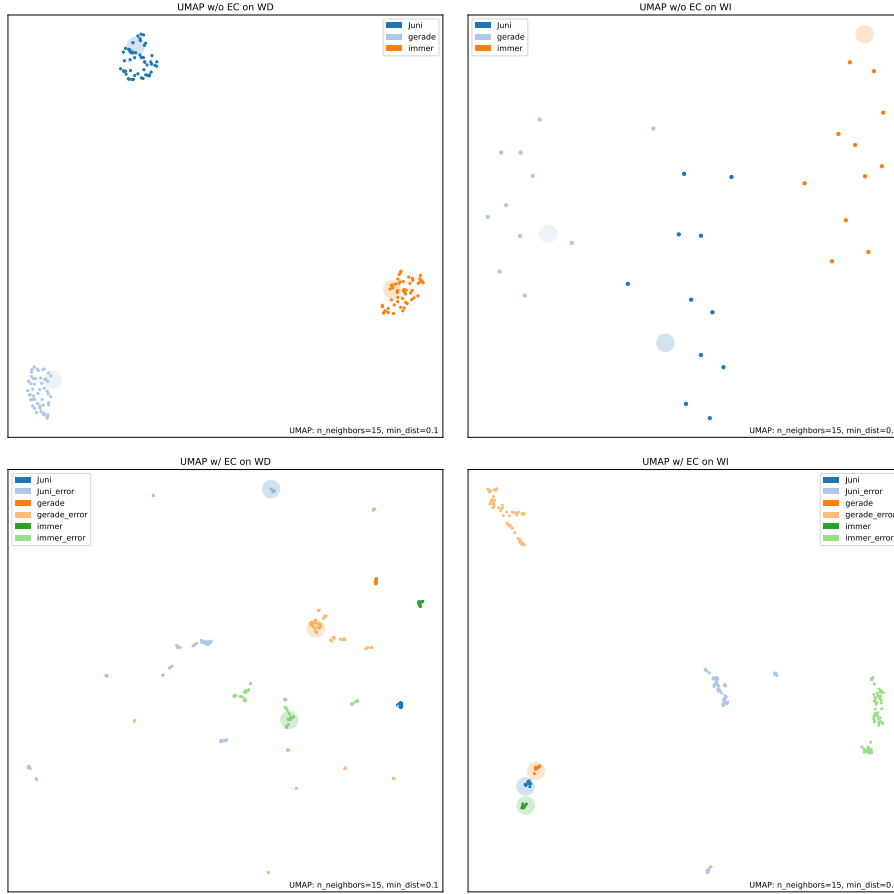


Fig. 3. UMAP Visualization of the Embedding Space. The plots display projected embeddings of sensor sequences (small dots), ground-truth text anchors (large transparent circles), and hard negative errors (faded dots). The top row shows baseline embeddings from models trained with the BC objective only, while the bottom row illustrates the impact of adding the EC objective.

The visualization highlights a distinct structural divergence between the two generalization tasks. In the baseline configurations without EC, the sensor embeddings generally form cohesive clusters that align with their corresponding

ground-truth text anchors. This indicates that the CTC and BC objectives provide effective modality alignment.

The impact of the EC objective is most evident in the second row. For the WI split, where the vocabulary is known but the writers are new, the EC objective successfully enforces a safety margin. The embeddings of hard negatives are pushed significantly away from the true positive clusters. This explicit separation reduces ambiguity and ensures that valid handwriting trajectories are not confused with fine-grained typos, which explains the superior performance of EC on the WI split.

In contrast, the WD split reveals why the EC objective is less effective for unseen vocabulary. Here, we observe a significant misalignment between the text anchors and their corresponding sensor sequence clusters. This discrepancy arises because the text encoder, having been trained on a specific character distribution, struggles to generalize its embeddings to the unseen word combinations in the validation set. This confirms our hypothesis that the flexible alignment of BC is preferred for the WD split, whereas the rigid discrimination of EC requires the stable anchors found in known vocabulary.

5 Conclusion & Outlook

In this work, we presented ECHWR, a novel training framework designed to enhance IMU-based *online* handwriting recognition. By introducing a temporary auxiliary branch and a dual contrastive objective, we enable standard encoder-decoder models to learn richer, more discriminative representations. Crucially, this improvement is achieved without modifying the baseline OnHWR model or incurring additional computational costs during inference. Our experiments on the OnHW-Words500 dataset demonstrate that ECHWR significantly outperforms state-of-the-art baselines while maintaining the exact same inference latency as the base model.

Our ablation studies reveal a critical dichotomy between different generalization tasks. We found that the WD task, which requires generalizing to unseen vocabulary, benefits most from the feature stability provided by RMS normalization and BC alignment. In contrast, the WI task is dominated by the variance of unseen writers. This scenario demands the robustness of layer normalization with registers and the fine-grained discrimination enforced by the EC objective.

Looking forward, we acknowledge that this study is limited by the current dataset size. This constraint prevented the identification of a universal configuration capable of simultaneously handling both writing style variations and character distribution shifts. Future work should address this limitation by leveraging larger-scale datasets with more complex vocabularies to determine whether a unified architecture can bridge this gap. Finally, given its general design, the ECHWR framework could potentially be useful for many other sequence recognition tasks beyond handwriting, such as acoustic speech recognition and optical character recognition.

A Visualization of Character Distribution

As demonstrated in Fig. 4, the character distributions of the WD and WI splits in the OnHWR-words500 dataset differ significantly.

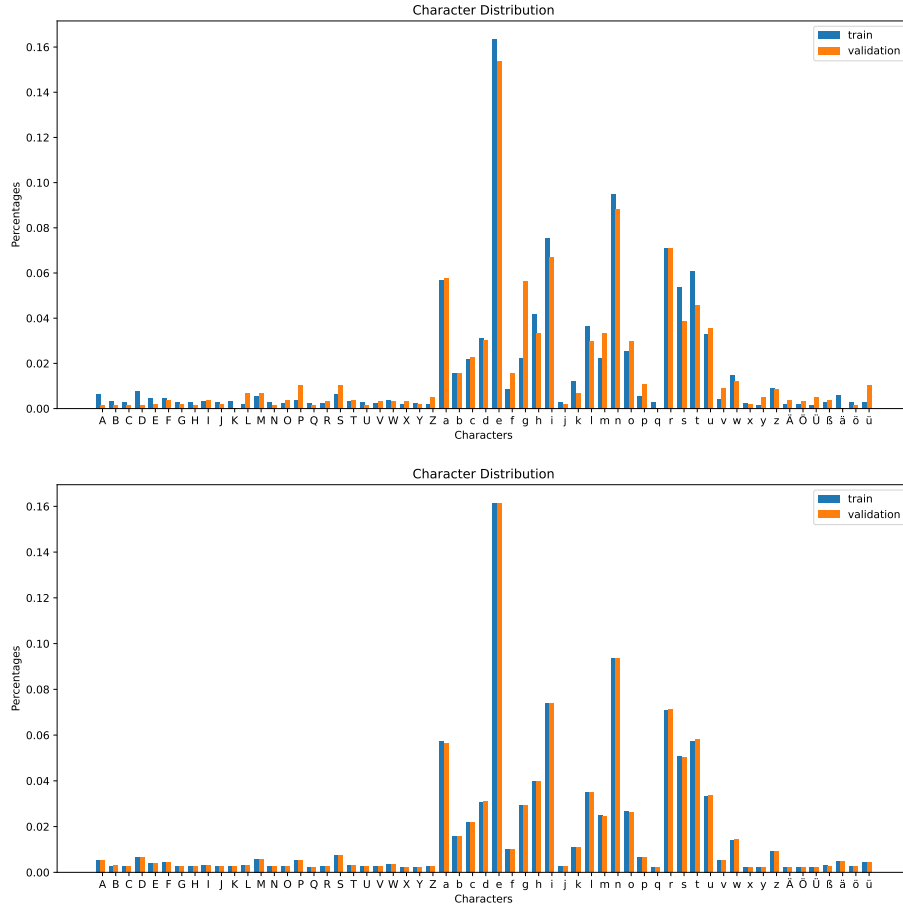


Fig. 4. Character distribution of the right-handed OnHW Words500 dataset. The upper and lower plots show the character distributions for the first fold of the WD and WI splits, respectively. Blue bars represent character frequencies in the training sets, while orange bars represent frequencies in the validation sets.

In the WI split (lower), the distributions between the training and validation sets match almost perfectly. Furthermore, each character is represented by at least a few data samples in both sets. In contrast, the distributions for the WD split (upper) vary greatly between the training and validation sets. Certain characters, such as “q” and “ä”, do not appear in the validation set at all.

References

1. Amma, C., Georgi, M., Schultz, T.: Airwriting: Hands-free mobile text input by spotting and continuous recognition of 3d-space handwriting with inertial sensors. In: 2012 16th International Symposium on Wearable Computers. pp. 52–59 (2012). <https://doi.org/10.1109/ISWC.2012.21>
2. Chen, T., Kornblith, S., Norouzi, M., Hinton, G.: A simple framework for contrastive learning of visual representations. In: Proceedings of the 37th International Conference on Machine Learning, ICML'20, JMLR.org (2020)
3. Choi, S.d., Lee, A.S., Lee, S.y.: On-line handwritten character recognition with 3d accelerometer. In: 2006 IEEE International Conference on Information Acquisition. pp. 845–850 (2006). <https://doi.org/10.1109/ICIA.2006.305842>
4. Darcret, T., Oquab, M., Mairal, J., Bojanowski, P.: Vision transformers need registers. In: The Twelfth International Conference on Learning Representations (2024), <https://openreview.net/forum?id=2dnO3LLiJ1>
5. Eldele, E., Ragab, M., Chen, Z., Wu, M., Kwoh, C.K., Li, X., Guan, C.: Time-series representation learning via temporal and contextual contrasting. In: Proceedings of the Thirtieth International Joint Conference on Artificial Intelligence, IJCAI-21. pp. 2352–2359 (2021)
6. Faundez-Zanuy, M., Mekyska, J.: Privacy of online handwriting biometrics related to biomedical analysis, chap. Chapter 2, pp. 17–39. IET (2017). https://doi.org/10.1049/PBSE004E_ch2, https://digital-library.theiet.org/doi/abs/10.1049/PBSE004E_ch2
7. Guo, P., Nakayama, M.: Towards user-generalizable wearable-sensor-based human activity recognition: A multi-task contrastive learning approach. Sensors **25**(22) (2025). <https://doi.org/10.3390/s25226988>, <https://www.mdpi.com/1424-8220/25/22/6988>
8. Hsu, Y.L., Chu, C.L., Tsai, Y.J., Wang, J.S.: An inertial pen with dynamic time warping recognizer for handwriting and gesture recognition. IEEE Sensors Journal **15**(1), 154–163 (2015). <https://doi.org/10.1109/JSEN.2014.2339843>
9. Jeen-Shing, W., Yu-Liang, H., Cheng-Ling, C.: Online handwriting recognition using an accelerometer-based pen device. In: Proceedings of the 2nd International Conference on Advances in Computer Science and Engineering (CSE 2013). pp. 231–234. Atlantis Press (2013). <https://doi.org/10.2991/cse.2013.52>, <https://doi.org/10.2991/cse.2013.52>
10. Jiang, R., Nguyen, T., Ishwar, P., Aeron, S.: Supervised contrastive learning with hard negative samples. In: 2024 International Joint Conference on Neural Networks (IJCNN). pp. 1–8 (2024). <https://doi.org/10.1109/IJCNN60899.2024.10650863>
11. Kalantidis, Y., Sariyildiz, M.B., Pion, N., Weinzaepfel, P., Larlus, D.: Hard negative mixing for contrastive learning. In: Proceedings of the 34th International Conference on Neural Information Processing Systems. NIPS '20, Curran Associates Inc., Red Hook, NY, USA (2020)
12. Khaertdinov, B., Asteriadis, S.: Temporal feature alignment in contrastive self-supervised learning for human activity recognition. In: 2022 IEEE International Joint Conference on Biometrics (IJCB). pp. 1–9 (2022). <https://doi.org/10.1109/IJCB54206.2022.10007984>
13. Kiyasseh, D., Zhu, T., Clifton, D.A.: Clocs: Contrastive learning of cardiac signals across space, time, and patients. In: International Conference on Machine Learning. pp. 5606–5615. PMLR (2021)

14. Li, J., Hamann, T., Barth, J., Kämpf, P., Zanca, D., Eskofier, B.: Robust and efficient writer-independent imu-based handwriting recognition. In: Durmaz Incel, Ö., Qin, J., Bieber, G., Kuijper, A. (eds.) *Sensor-Based Activity Recognition and Artificial Intelligence*. pp. 261–286. Springer Nature Switzerland, Cham (2026)
15. Li, M., Lv, T., Chen, J., Cui, L., Lu, Y., Florencio, D., Zhang, C., Li, Z., Wei, F.: Trocr: transformer-based optical character recognition with pre-trained models. In: *Proceedings of the Thirty-Seventh AAAI Conference on Artificial Intelligence and Thirty-Fifth Conference on Innovative Applications of Artificial Intelligence and Thirteenth Symposium on Educational Advances in Artificial Intelligence. AAAI'23/IAAI'23/EAAI'23*, AAAI Press (2023). <https://doi.org/10.1609/aaai.v37i11.26538>, <https://doi.org/10.1609/aaai.v37i11.26538>
16. Li, Y., Chen, D., Tang, T., Shen, X.: Htr-vt: Handwritten text recognition with vision transformer. *Pattern Recognition* **158**, 110967 (2025). <https://doi.org/https://doi.org/10.1016/j.patcog.2024.110967>, <https://www.sciencedirect.com/science/article/pii/S0031320324007180>
17. Liu, X., Liang, Y., Huang, C., Zheng, Y., Hooi, B., Zimmermann, R.: When do contrastive learning signals help spatio-temporal graph forecasting? In: *Proceedings of the 30th International Conference on Advances in Geographic Information Systems. SIGSPATIAL '22*, Association for Computing Machinery, New York, NY, USA (2022). <https://doi.org/10.1145/3557915.3560939>, <https://doi.org/10.1145/3557915.3560939>
18. McInnes, L., Healy, J., Saul, N., Großberger, L.: Umap: Uniform manifold approximation and projection. *Journal of Open Source Software* **3**(29), 861 (2018). <https://doi.org/10.21105/joss.00861>, <https://doi.org/10.21105/joss.00861>
19. Ott, F., Rügamer, D., Heublein, L., Hamann, T., Barth, J., Bischl, B., Mutschler, C.: Benchmarking online sequence-to-sequence and character-based handwriting recognition from imu-enhanced pens. *Int. J. Doc. Anal. Recognit.* **25**(4), 385–414 (Dec 2022). <https://doi.org/10.1007/s10032-022-00415-6>, <https://doi.org/10.1007/s10032-022-00415-6>
20. Qiu, Z., Wang, Z., Zheng, B., Huang, Z., Wen, K., Yang, S., Men, R., Yu, L., Huang, F., Huang, S., Liu, D., Zhou, J., Lin, J.: Gated attention for large language models: Non-linearity, sparsity, and attention-sink-free. In: *The Thirty-ninth Annual Conference on Neural Information Processing Systems* (2025), <https://openreview.net/forum?id=1b7whO4SFY>
21. Radford, A., Kim, J.W., Hallacy, C., Ramesh, A., Goh, G., Agarwal, S., Sastry, G., Askell, A., Mishkin, P., Clark, J., Krueger, G., Sutskever, I.: Learning transferable visual models from natural language supervision (2021), <https://arxiv.org/abs/2103.00020>
22. Robinson, J.D., Chuang, C.Y., Sra, S., Jegelka, S.: Contrastive learning with hard negative samples. In: *International Conference on Learning Representations* (2021), <https://openreview.net/forum?id=CR1XOQ0UTH>
23. Vaswani, A., Shazeer, N., Parmar, N., Uszkoreit, J., Jones, L., Gomez, A.N., Kaiser, L.u., Polosukhin, I.: Attention is all you need. In: Guyon, I., Luxburg, U.V., Bengio, S., Wallach, H., Fergus, R., Vishwanathan, S., Garnett, R. (eds.) *Advances in Neural Information Processing Systems. vol. 30*. Curran Associates, Inc. (2017), https://proceedings.neurips.cc/paper_files/paper/2017/file/3f5ee243547dee91fbd053c1c4a845aa-Paper.pdf
24. Wehbi, M., Hamann, T., Barth, J., Kaempf, P., Zanca, D., Eskofier, B.: Towards an imu-based pen online handwriting recognizer. In: Lladós, J., Lopresti, D., Uchida, S. (eds.) *Document Analysis and Recognition – ICDAR 2021*. pp. 289–

303. Springer International Publishing, Cham (2021). https://doi.org/10.1007/978-3-030-86334-0_19
25. Yousef, M., Bishop, T.E.: Origaminet: Weakly-supervised, segmentation-free, one-step, full page text recognition by learning to unfold. In: 2020 IEEE/CVF Conference on Computer Vision and Pattern Recognition (CVPR). pp. 14698–14707 (2020). <https://doi.org/10.1109/CVPR42600.2020.01472>
26. Zhang, B., Sennrich, R.: Root mean square layer normalization. In: Wallach, H., Larochelle, H., Beygelzimer, A., d'Alché-Buc, F., Fox, E., Garnett, R. (eds.) Advances in Neural Information Processing Systems. vol. 32. Curran Associates, Inc. (2019), https://proceedings.neurips.cc/paper_files/paper/2019/file/1e8a19426224ca89e83cef47f1e7f53b-Paper.pdf
27. Zhang, P., Liu, Y., Lai, S., Li, H., Jin, L.: Privacy-preserving biometric verification with handwritten random digit string. IEEE Transactions on Pattern Analysis and Machine Intelligence **47**(4), 3049–3066 (2025). <https://doi.org/10.1109/TPAMI.2025.3529022>
28. Zhang, X., Zhao, Z., Tsiligkaridis, T., Zitnik, M.: Self-supervised contrastive pre-training for time series via time-frequency consistency. In: Proceedings of the 36th International Conference on Neural Information Processing Systems. NIPS '22, Curran Associates Inc., Red Hook, NY, USA (2022)